



**HAL**  
open science

## Significant role of iron on the fate and photodegradation of enrofloxacin

Iván Sciscenko, Antonio Arques, Zsuzsanna Varga, Stephane Bouchonnet,  
Olivier Monfort, Marcello Brigante, Gilles Mailhot

### ► To cite this version:

Iván Sciscenko, Antonio Arques, Zsuzsanna Varga, Stephane Bouchonnet, Olivier Monfort, et al.. Significant role of iron on the fate and photodegradation of enrofloxacin. *Chemosphere*, 2021, 270, pp.129791. 10.1016/j.chemosphere.2021.129791 . hal-03169173

**HAL Id: hal-03169173**

**<https://uca.hal.science/hal-03169173>**

Submitted on 15 Mar 2021

**HAL** is a multi-disciplinary open access archive for the deposit and dissemination of scientific research documents, whether they are published or not. The documents may come from teaching and research institutions in France or abroad, or from public or private research centers.

L'archive ouverte pluridisciplinaire **HAL**, est destinée au dépôt et à la diffusion de documents scientifiques de niveau recherche, publiés ou non, émanant des établissements d'enseignement et de recherche français ou étrangers, des laboratoires publics ou privés.



Distributed under a Creative Commons Attribution - NonCommercial - NoDerivatives 4.0 International License



## Significant role of iron on the fate and photodegradation of enrofloxacin



Iván Sciscenko<sup>b</sup>, Antonio Arques<sup>b</sup>, Zsuzsanna Varga<sup>c</sup>, Stephane Bouchonnet<sup>c</sup>, Olivier Monfort<sup>a,d</sup>, Marcello Brigante<sup>a</sup>, Gilles Mailhot<sup>a,\*</sup>

<sup>a</sup> Université Clermont Auvergne, CNRS, SIGMA Clermont, Institut de Chimie de Clermont-Ferrand, 63000, Clermont-Ferrand, France

<sup>b</sup> Departamento de Ingeniería Textil y Papelera, Universitat Politècnica de València, Alcoy, Spain

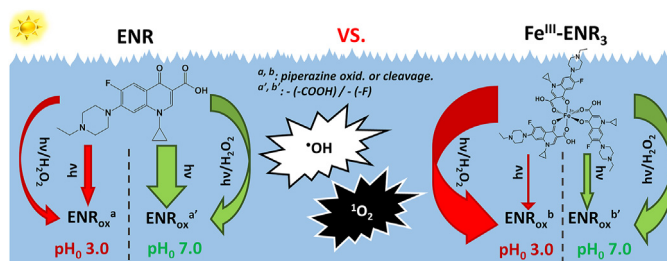
<sup>c</sup> Laboratoire de Chimie Moléculaire – CNRS / Ecole Polytechnique, IP Paris, 91128, Palaiseau, France

<sup>d</sup> Comenius University in Bratislava, Faculty of Natural Sciences, Department of Inorganic Chemistry, Ilkovicova 6, Mlynska Dolina, 84215, Bratislava, Slovakia

### HIGHLIGHTS

- Enrofloxacin-Fe(III) complex was formed and photolysed.
- Photolytic rate constants and photo-product formation, were pH and iron dependent.
- The effects of dissolved oxygen and H<sub>2</sub>O<sub>2</sub> addition were explored.
- Iron complexation notably diminished enrofloxacin photodegradation.

### GRAPHICAL ABSTRACT



### ARTICLE INFO

#### Article history:

Received 16 September 2020

Received in revised form

20 January 2021

Accepted 24 January 2021

Available online 27 January 2021

Handling Editor: Klaus Kümmeler

#### Keywords:

Fluoroquinolone

Iron complexation

Photo-fenton

Photolysis

Photoproducts identification

Self-sensitization

### ABSTRACT

Enrofloxacin (ENR) belongs to the fluoroquinolone (FQ) antibiotics family, which are contaminants of emerging concern frequently found in effluents. Although many works studying photo-Fenton process for FQ degradation have been reported, there are no reports analysing in deep the effect of iron complexation, as well as other metals, towards FQs' photolysis, which, evidently, also contributes in the overall degradation of the pollutant. Therefore, in this work, we report a comparative study between the photochemical fate of ENR and its complex with Fe(III) under simulated sunlight irradiation. In addition, the effect of dissolved oxygen, self-sensitization process, and H<sub>2</sub>O<sub>2</sub> addition on the studied photochemical systems are also investigated. Results indicate that, for free and iron-complexed ENR, singlet oxygen (<sup>1</sup>O<sub>2</sub>) is generated from the interaction of its triplet state with ground state oxygen. Half-life time (t<sub>1/2</sub>) of ENR under sun simulated conditions is estimated to be around 22 min, while complexation with iron enhances its photostability, leading to a t<sub>1/2</sub> of 2.1 h. Such finding indicates that at least the presence of iron, might notably increase the residence time of these pollutants in the environment. Eventually, only with the addition of H<sub>2</sub>O<sub>2</sub>, the FQ-iron complex is efficiently degraded due to photo-Fenton process even at circumneutral pH values due to the high stability of the formed complex. Finally, after LC/FT-ICR MS analysis, 39 photoproducts are detected, of which the 14 most abundant ones are identified. Results indicate that photoproducts formation is pH and iron dependent.

© 2021 The Authors. Published by Elsevier Ltd. This is an open access article under the CC BY-NC-ND license (<http://creativecommons.org/licenses/by-nc-nd/4.0/>).

**Abbreviations:** Enrofloxacin, ENR; fluoroquinolone(s), FQ(s); reactive oxygen species, ROS; isopropyl alcohol, IPA; furfuryl alcohol, FFA; ligand to metal charge transfer, LMCT; wastewater treatment plant, WWTP.

\* Corresponding author.

E-mail address: [gilles.mailhot@uca.fr](mailto:gilles.mailhot@uca.fr) (G. Mailhot).

<https://doi.org/10.1016/j.chemosphere.2021.129791>

0045-6535/© 2021 The Authors. Published by Elsevier Ltd. This is an open access article under the CC BY-NC-ND license (<http://creativecommons.org/licenses/by-nc-nd/4.0/>).

## 1. Introduction

Antibiotics are among the substances considered as contaminants of emerging concern; they are present in urban wastewater and they persist even after treatment in conventional wastewater treatment plants (WWTPs), this being an entry route into the environment (Kümmerer, 2009; Silva et al., 2011; Verlicchi et al., 2012). Within this category, fluoroquinolones (FQs), are one of the most consumed antibiotics of the world (Hamad, 2010).

FQs can absorb light within the range of solar radiation ( $\lambda > 300$  nm), and due to their abundance in natural effluents, photodegradation of these molecules had been thoroughly studied in order to have further insights related to their fate and photo-product formation in surface waters (Batchu et al., 2014; Ge et al., 2015; Haddad and Kümmerer, 2014). Besides, these compounds can easily interact with humic-like substances (Aristilde and Sposito, 2010), soil (Riaz et al., 2018), and even WWTP sludge, where they can accumulate (Van Doorslaer et al., 2014). In this regard, another water constituent to take into consideration are metals. FQs present high affinity to metal complexation. They can act as mono or bidentate ligands, as well as bridging ligand, being the most common coordination mode via carbonyl and carboxyl groups in adjacent positions (Uivarosi, 2013).

To date, however, there is a lack of information about the FQ-metal environmental behaviour, recently collected in the review of (Cuprys et al., 2018), where they reported significant changes towards their toxicity, soil-water mobility, WWTP degradation efficiencies and photochemistry. Regarding the latter, DFT calculations have shown that the complex formed between one of the most frequently found FQ in natural effluents, the enrofloxacin (ENR), with  $Mg^{2+}$ , presented higher activation energies for the most direct photolysis pathways than ENR itself (Wang et al., 2018). Similarly for ciprofloxacin, another highly consumed FQ, which is also the main photoproduct of ENR (Snowberger et al., 2016), in presence of Cu(II) exhibited a strong photolytic inhibition, only recovered in presence of ethylenediaminetetraacetic acid (EDTA) (Wei et al., 2015). On the contrary, Cu(II) increased by a factor of 2.4 the photolytic rate constant of moxifloxacin (Hubicka et al., 2012), thus indicating that FQ-metal photochemical behaviour could also be dependent on the antibiotic molecular structure.

Advanced oxidation processes (AOPs) had long been studied and proposed for tertiary wastewater treatment, as they are able to degrade these emerging pollutants (Salimi et al., 2017). In one of the most common AOP, the Fenton process, the highly reactive species  $\cdot OH$  and  $HO_2\cdot$  involved in the contaminants abatement, are formed in the elementary reactions of  $H_2O_2$  disproportionation catalyzed by Fe(II)/Fe(III) (and other transition metals) and enhanced by the action of light (photo-Fenton) (Pignatello et al., 2006), which could be also photogenerated *in situ* in the natural environment (Vermilyea and Voelker, 2009). In these cases, when the pollutant is also photolabile, photolysis degradation contribution must be also considered. However, although many studies of FQs oxidation by photo-Fenton had been published (Gou et al., 2020), the individual effect of iron towards FQs' photochemical fate is practically unexplored. For instance (Qju et al., 2019), when treated two FQs and another type of antibiotic by UV/Fe(III), it can be seen that for the tested FQs, its removal rate was much more sensitive to the iron concentration variation compared to the other non-FQ antibiotic. According to the above mentioned statements, this could had been most likely related to the downplayed FQ-iron interaction, not present in the case of the other compound. In this regard, FQs Fenton degradation has been reported as effective even at mild pH conditions due to iron chelation by the pollutant itself (Sciscenko et al., 2020).

In this work, we decided to compare the photochemical fate

under sun-simulated conditions of a model FQ (ENR) alone and as Fe(III)-complex. First, spectroscopic characterization and stability of the complex between ENR and Fe(III) was assessed, secondly, photochemical degradation of ENR and its Fe(III)-complex was evaluated with and without addition of hydrogen peroxide. Finally, the main photoproducts were characterized, and a schematic degradation pathway was proposed. Besides the environmental aspect, we believe that these results will be useful to better comprehend the behaviour of FQs degradation by photo-Fenton and analogues processes.

## 2. Materials and methods

### 2.1. Reagents and chemical analysis

Reagents, chemical analysis and kinetics methods are described in the Supporting Information. For further information about transition absorption experiments using laser flash photolysis system, this equipment and procedure have been described in previously published papers (Huang et al., 2018; Tao et al., 2019). When specified, filtration was performed employing Chromafil Xtra PTFE 0.45  $\mu m$  filters and no significant ENR retention (i.e. adsorption on the filter) was determined. All the solutions were prepared with ultra-pure water (18.2 M $\Omega$  cm).

### 2.2. Fe-ENR complex characterization

The complex formation between Fe(III) and ENR was studied by analysing its stoichiometry and pH-stability. Fe-ENR stoichiometry was obtained by applying the method of continuous variation (Renny et al., 2013), acquiring the UV-vis spectra of fixed 100  $\mu M$  Fe(III) solution at pH 3.0 with different ENR concentrations in the range 100–600  $\mu M$ . For pH-stability analysis, the complex between ENR and Fe(III) was firstly prepared at pH 3.0, and afterwards, pH was increased until the desired value and leaving each solution for 10 h in the dark with magnetic stirring.

### 2.3. Irradiation experiments and analysis

Photochemical experiments were carried out in a thermostat cylindrical open glass reactor (total volume of 50 mL) at 20 °C loaded with 25 mL of the testing solution containing ENR 300  $\mu M$ , with and without Fe(III) 100  $\mu M$ . Irradiations were performed with a solar simulator (Lot-Oriel LS0306) equipped with a high-pressure Xe short arc lamp (Ushio UXL-302-O) and a Pyrex filter to avoid wavelengths < 290 nm. Iron-ENR complex solutions were always prepared and left with stirring for at least 10 h to assure full complexation prior to irradiation experiments. All assays were performed for 2 h, withdrawing 1 mL of sample in time-intervals and filtered with PTFE 0.45  $\mu m$  Chromafil Xtra filters. When needed, 200  $\mu M$   $H_2O_2$  were employed as source of  $\cdot OH$ . Two initial pH were studied, 3.0 where Fenton-(like) processes are optimal, and 7.0, relevant towards realistic natural/wastewater scenario. All samples (1 mL) were filtered with PTFE 0.45  $\mu m$  filters and mixed with 100  $\mu L$  of methanol in order to stop the reaction before analysis (i.e. to quench possible hydroxyl radical formation through Fenton reaction). Experiments were performed at least twice.

The oxygen effect was studied by bubbling solution with pure  $N_2$  and  $O_2$  for 10 min before and during the photochemical experiment, thus assuring negligible and high  $O_2$  concentrations, respectively. Formation of reactive oxygen species (ROS) was studied employing isopropyl alcohol (IPA) ( $\cdot OH$  scavenger,  $k(\cdot OH) = 1.9 \times 10^9 M^{-1} s^{-1}$ ) and furfuryl alcohol (FFA) ( $\cdot OH$  and  $^1O_2$  scavenger,  $k(\cdot OH) = 1.5 \times 10^{10} M^{-1} s^{-1}$  and  $k(^1O_2) = 1.2 \times 10^8 M^{-1} s^{-1}$ , respectively) (Buxton et al., 1988; Haag et al.,

1984). IPA was employed in a concentration of 5 mM whereas FFA of 300  $\mu\text{M}$ . The chosen concentrations were based on other related works (Bokare and Choi, 2015; Latch et al., 2003; Zhang et al., 2019), ROS being able to react much faster with the probes than with ENR at 300  $\mu\text{M}$ . It is important to highlight that FFA was chosen over  $\text{NaN}_3$  as  $^1\text{O}_2$  probe since this last one is highly pH dependent ( $k(^1\text{O}_2)(\text{N}_3^-) = 5 \times 10^8 \text{ M}^{-1} \text{ s}^{-1}$  and  $k(^1\text{O}_2)(\text{HN}_3) \approx 1 \times 10^6 \text{ M}^{-1} \text{ s}^{-1}$ , with  $\text{pK}_a = 4.6$ , being also  $\text{HN}_3$  strongly partitioned to the gas phase) (Haag and Mill, 1987), whereas FFA is not (Appiani et al., 2017), thus being better when comparing assays at pH 3.0 with pH 7.0.

### 3. Results and discussion

#### 3.1. Complexation with ferric ions

When iron (III) perchlorate is added to an ENR solution (both colourless) at pH 3.0, the mixture changed into a yellow-colour solution. Indeed, an absorbance shoulder after 400 nm and up to 540 nm appears in the UV–vis spectrum of ENR-iron mixture (Fig. 1A). Such absorption suggests that a charge-transfer transition between the ENR and Fe(III) occurs, corresponding to the formation of a coordination complex (Efthimiadou et al., 2008). In Fig. 1B, the absorbance at 430 nm as a function of different ENR/Fe(III) ratios is depicted. Absorbance increases from 0.23 to about 0.43 when ENR/Fe(III) ratio grows up to 3, and then reaches a plateau at higher

ratios. Such finding is in agreement with an octahedral complex employing the FQ carbonyl and carboxyl moieties to bind Fe(III) with a ratio 3:1, which has been previously reported (Urbaniak and Kokot, 2009).

Then, the ENR-iron complex ( $\text{Fe}^{\text{III}}\text{-ENR}_3$ ) stability was investigated in the range of pH 3.0 to 9.0 with measuring the total iron concentration in solution. Fig. 1C shows that dissolved Fe(III) concentration remained constant for pH values below 7.5, while for  $\text{pH} \geq 8.0$ , a decay due to precipitation of its (oxy)hydroxides was observed (Stefánsson, 2007). However, measurements without filtration have shown that Fe(III) concentration remained at ca. 100  $\mu\text{M}$  even until pH 9.0, indicating that ENR is also capable of stabilizing Fe(III) in the colloidal state.

In addition,  $\text{Fe}^{\text{III}}\text{-ENR}_3$  solutions from pH 3.0 to 7.5 proved to be stable at least for one month in the dark and at room temperature since Fe(III) remained in solution all time. In fact, the formation constant of  $\text{Fe}^{\text{III}}\text{-ENR}_3$  complex is reported to have its highest value at acidic pH,  $\log K(\text{Fe}^{\text{III}}\text{-ENR}_3) \approx 45$ , and it decreases with increasing pH, being equal to 25 at neutral conditions (Urbaniak and Kokot, 2009). These values are comparable with other stable Fe(III)-organic ligand complexes such as EDTA ( $\log K(\text{Fe}^{\text{III}}\text{-EDTA}) \approx 25$ ) (Bucheli-Witschel and Egli, 2001).

Preparation of analogous solutions containing Fe(II) instead of Fe(III) did not evidence the complex signal at 430 nm, thus indicating that the ENR-ferrous complex is not formed (Chen et al., 2017).

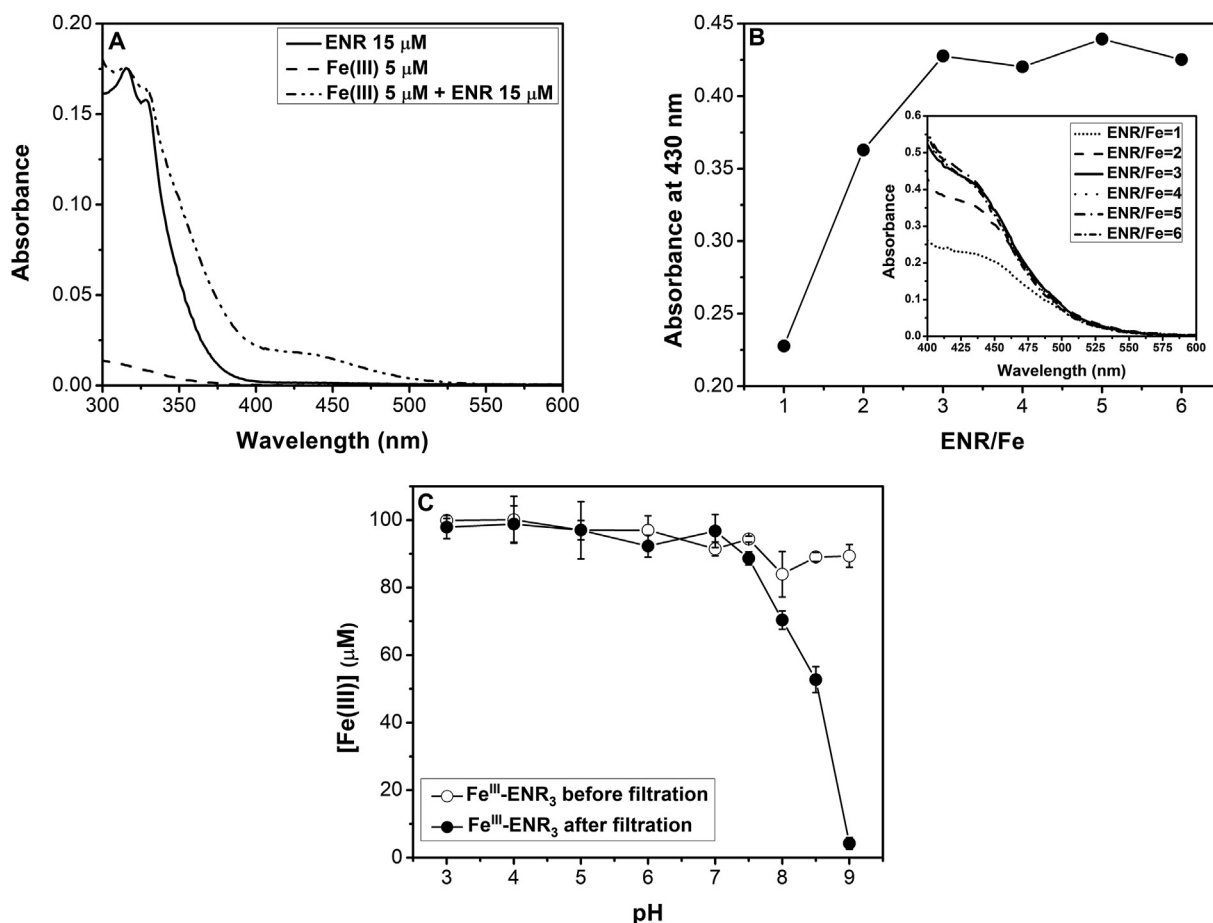


**Fig. 1.** (A) Absorption spectra for ENR, Fe(III) and  $\text{Fe}^{\text{III}}\text{-ENR}_3$  at pH 3.0; (B) Method of continuous variation for a fixed amount of Fe(III) 100  $\mu\text{M}$  and varying ENR concentration from 100 to 600  $\mu\text{M}$ . Insert represent the UV–vis spectra of different ENR/Fe(III) ratio solutions at pH 3.0. (C) Fe(III) concentration from 100  $\mu\text{M}$   $\text{Fe}^{\text{III}}\text{-ENR}_3$  complex at different pH values measured 24 h after preparation. PTFE filters 0.45  $\mu\text{m}$  were used to filter solutions. Values represent the average of two measurements, and the error bar gives the associated uncertainty.

### 3.2. Photodegradation experiments

#### 3.2.1. Effect of pH

In order to investigate the degradation of the antibiotic, in free form or as iron-complex, the same concentration of ENR was considered for all the experiments (300  $\mu\text{M}$  of ENR or 100  $\mu\text{M}$  of  $\text{Fe}^{\text{III}}\text{-ENR}_3$ ) in acidic (pH 3.0) and neutral (pH 7.0) solutions (Fig. 2A). In this way, even though the pollutant concentration was higher than the environmental related levels, this allowed us to also study the  $\text{Fe}(\text{III})/\text{Fe}(\text{II})$  behaviour (see later Fig. 3B and S5). In addition, the concentrations of the complex  $\text{Fe}^{\text{III}}\text{-ENR}_3$  between 1 and 100  $\text{mg L}^{-1}$  has no effect on the photochemical process. Besides, some studies propose the use of photo-Fenton to treat the concentrate stream from membrane processes, hence, dealing with higher concentration of pollutants (Miralles-Cuevas et al., 2014).

Under irradiation at pH 3.0, the pseudo-first order photolysis rate constants of ENR and as iron-complex were  $3.7 \times 10^{-3}$  and  $2.0 \times 10^{-3} \text{ min}^{-1}$ , respectively. Therefore, even though  $\text{Fe}^{\text{III}}\text{-ENR}_3$  exhibited greater absorbance within the visible region, we can assume that this complex could present higher activation energy for most of the photodegradation pathways of ENR, hence, being more stable against light irradiation than the pollutant alone, as it has been reported for other FQ-metal complexes (Wang et al., 2018; Wei et al., 2015). At pH 7.0, where the zwitterionic form of ENR becomes predominant ( $\text{pK}_{\text{a}1} \approx 6.0$  and  $\text{pK}_{\text{a}2} \approx 8.5$ , Fig. S1), the photolysis rate constant was one order of magnitude higher than at acidic conditions ( $k_{\text{ENR}} = 3.1 \times 10^{-2} \text{ min}^{-1}$ ), which is in agreement with the higher photolysis quantum yields of FQs for zwitterionic forms associated to changes in functional groups reactivity with the ionic forms (Ge et al., 2018). After 2 h of irradiation, the pH decreased to 6.0 due to decarboxylation of the molecule, as confirmed by mass spectrometry analysis (section 3.4). Interestingly, in the case of iron-complex, the photolysis enhancement was clearly less marked than for free antibiotic, being its kinetic rate constant  $5.3 \times 10^{-3} \text{ min}^{-1}$ , only 2.7 times more than at pH 3.0.

It is important to highlight that photolysis results at pH 3.0 could had also been well explained by zero order fitting (see Figs. S2A–B). However, this is opposed to the consensus of photolytic pseudo-first order kinetic fitting for FQs in all previously cited related works employing ca. 5  $\mu\text{M}$  (Zhang et al., 2019), 120  $\mu\text{M}$  (Li et al., 2011) or even  $2.78 \times 10^3 \mu\text{M}$  (Qiu et al., 2019).

#### 3.2.2. ROS generation and effect of dissolved oxygen

In order to understand the degradation mechanisms, different photochemical experiments were performed in the presence of ROS scavengers, such as IPA and FFA, or in oxygen saturated and de-aerated solutions. As shown in Fig. S2, the presence of IPA (5 mM) and FFA (300  $\mu\text{M}$ ) did not significantly modify the degradation of ENR or  $\text{Fe}^{\text{III}}\text{-ENR}_3$ , indicating that generation of  $\cdot\text{OH}$  or  $^1\text{O}_2$  by the self-sensitization process should not be relevant for ENR degradation in any of the studied cases. However,  $^1\text{O}_2$  generation was confirmed when observing FFA degradation (Fig. S3). At both studied pH, a 40% FFA removal was obtained after 120 min with ENR, whereas for  $\text{Fe}^{\text{III}}\text{-ENR}_3$ , 10% and 25% was obtained at pH values 3.0 and 7.0, respectively. Therefore,  $^1\text{O}_2$  formation should be reduced when ENR is chelating  $\text{Fe}(\text{III})$ , which is in agreement with other FQ-metal complexes that showed a decrease in singlet oxygen overall production (Albini and Monti, 2003). Nevertheless, this could be also linked to the slower photolysis degradation in the case of the complex, resulting also in a lower singlet oxygen production. Therefore, we can conclude that  $\text{Fe}(\text{III})$  complexation by ENR should affect more its direct photolysis pathways rather than its photosensitized ones.

Although singlet oxygen is formed through the interaction of dissolved oxygen ( $^3\text{O}_2$ ) with the excited states of other molecules (Niu et al., 2018), ENR photodegradation was slower when increasing the amount of dissolved oxygen in the system. For instance, at pH = 3.0 and with the antibiotic alone, a photolytic rate constant of  $4.8 \times 10^{-3} \text{ min}^{-1}$  was determined under de-aerated conditions, whereas with an oxygen-saturated solution was  $1.9 \times 10^{-3} \text{ min}^{-1}$  (Fig. 2A). In line with these observations, faster quenching of ENR triplet state ( $\text{ENR}^*$ ) was obtained when increasing the dissolved oxygen concentration (Fig. 2B). Therefore, even though ENR could be oxidized by photogenerated  $^1\text{O}_2$ , the reactivity between them is estimated to be around  $10^6 \text{ M}^{-1} \text{ s}^{-1}$  (Albini and Monti, 2003), which is considerably lower than the  $^3\text{O}_2$  quenching by  $\text{ENR}^*$ , determined to be 4.7 and  $3.7 \times 10^9 \text{ M}^{-1} \text{ s}^{-1}$  at pH 3 (Fig. S4A) and 7 (Fig. 2B), respectively. For  $\text{Fe}^{\text{III}}\text{-ENR}_3$ , the same counterproductive effect of ground state dissolved oxygen was observed, with the difference that the obtained removals were proportionally slower than the antibiotic in free form, in agreement with the higher photochemical stability of the FQ-metal complex.

At pH 7.0, dissolved oxygen inhibitory effect for ENR was observed when comparing aerated/de-aerated conditions

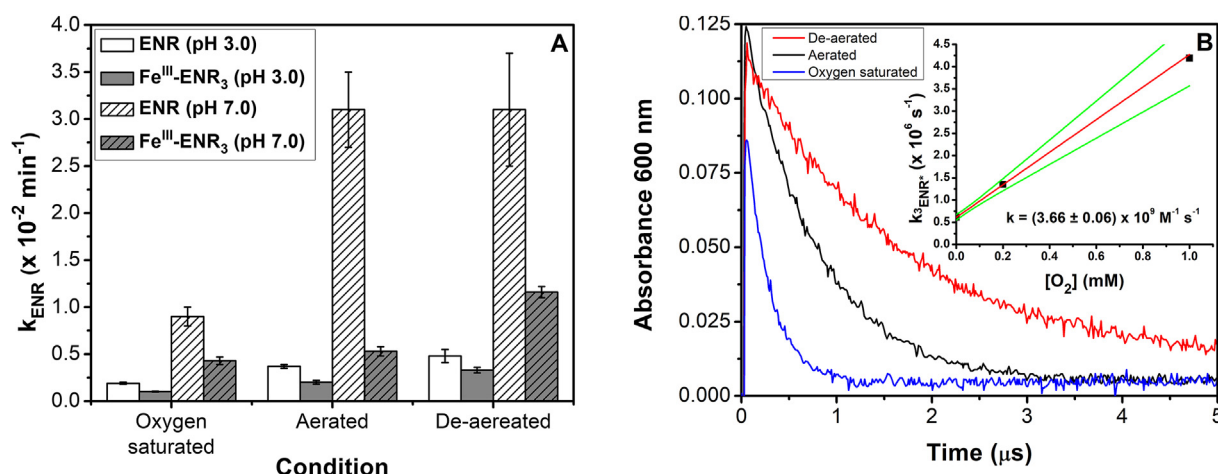


**Fig. 2.** (A) Photolytic rate constants for ENR 300  $\mu\text{M}$  and  $\text{Fe}^{\text{III}}\text{-ENR}_3$  100  $\mu\text{M}$  at all tested conditions (error bars were calculated from the deviation from linear fit and experimental data); (B)  $^3\text{ENR}^*$  relaxation kinetics from ENR 280  $\mu\text{M}$  at pH 7.0 by laser flash photolysis measurements at de-aerated, aerated and oxygen saturated conditions. In the insert,  $^3\text{O}_2$  quenching kinetic rate constant determination from obtained relaxation fitting curves.

( $k_{\text{ENR}} = 3.1 \times 10^{-2} \text{ min}^{-1}$  in both cases) against oxygen-saturated ones ( $k_{\text{ENR}} = 9 \times 10^{-3} \text{ min}^{-1}$ ). On the contrary, for  $\text{Fe}^{\text{III}}\text{-ENR}_3$ , the tendency remained as at acidic conditions, observing decreasing photolytic rate constants when going from de-aerated towards aerated, and oxygen saturated conditions (Fig. 2A).

$\text{Fe}(\text{II})$  formation due to ligand to metal charge transfer (LMCT) within the photolysis of  $\text{Fe}^{\text{III}}\text{-ENR}_3$  at pH 3.0, followed the same tendency, de-aerated > aerated > oxygen saturated (Fig. S5), obtaining after 60 min irradiation, a reduction of 100% from  $\text{Fe}(\text{III})$  to  $\text{Fe}(\text{II})$  with  $\text{N}_2$  bubbling, 87% in aerated conditions, and 36% with  $\text{O}_2$  bubbling.

Based on these results, a plausible reaction mechanism can be proposed as following: after absorption of light, an electron of ENR can be promoted to the excited state ( $^1\text{ENR}^*$ ) followed by intersystem crossing and generation of ENR triplet state ( $^3\text{ENR}^*$ ) (Eq (1)). The excited triplet state can lead to the formation of degradation product (Eq (2)) or can be quenched by molecular oxygen ( $^3\text{O}_2$ ) through energy transfer reaction leading to the formation of singlet oxygen ( $^1\text{O}_2$ ) and ENR ground state (Eq (3)). Photogenerated  $^1\text{O}_2$  can also slightly contribute to the oxidation of ENR (Eq (4)).



For  $\text{Fe}^{\text{III}}\text{-ENR}_3$ , the first photoinduced reaction is the LMCT reaction, leading to the formation of ferrous ions ( $\text{Fe}(\text{II})$ ), 2 molecules of ENR, and ENR radical ( $\text{ENR}^*$ ) in solution (Eq (5)).  $\text{ENR}^*$  can start different degradation pathways in which water and oxygen can be involved (Eq (6)).



### 3.2.3. Time-course absorbance spectra changes

Analysing the changes in absorbance spectra with light irradiation for ENR and  $\text{Fe}^{\text{III}}\text{-ENR}_3$  at pH 3.0, a signal formation at 535 nm

was observed (Fig. 3A and B), also evidenced by a final light pink colour of the solutions after the 120 min of irradiation, which could probably be related to the formation of poly-conjugated products (Sturini et al., 2010). Secondly, analysing the iron complex (Fig. 3B) two additional issues have been seen: 1) there is a decay in 430 nm complex signal, which is related to the  $\text{Fe}(\text{III})$  reduction to  $\text{Fe}(\text{II})$  due to LMCT process, and 2) an isosbestic point at 516 nm was obtained, which suggests the conversion of  $\text{Fe}^{\text{III}}\text{-ENR}_3$  into one main absorbing photoproduct.

Analogous results for pH 7.0 are shown in Figs. S6A–B, where pink colourization of the solution after irradiation was also observed, thus, with signal formation at 535 nm (however, not as pronounced as at acidic conditions). As expected, no complex absorbance signal decay was observed for  $\text{Fe}^{\text{III}}\text{-ENR}_3$  due to fast re-oxidation of  $\text{Fe}(\text{II})$  at neutral pH. In addition, there was only a negligible dissolved total iron loss within  $\text{Fe}^{\text{III}}\text{-ENR}_3$  irradiations at pH 7.0 (5–10% after 2 h), indicating that the by-product formation should be of the FQ-type structure, hence still being capable of binding iron and keeping it in aqueous solution even at neutral pH (Sciscenko et al., 2020).

### 3.3. Impact of $\text{H}_2\text{O}_2$ addition

In the frame of water treatment, the effect of  $\text{H}_2\text{O}_2$  addition (200  $\mu\text{M}$ ) was also studied. In this case, higher amounts of  $\cdot\text{OH}$  are produced *in situ* due to  $\text{H}_2\text{O}_2$  photolysis observed using the same irradiation setup (Eq (7)) (Bianco et al., 2015) as well as Fenton-like and Fenton reactions (Eqs (8) and (9)), strongly enhanced by the photo-generated  $\text{Fe}(\text{II})$  in the presence of the complex  $\text{Fe}^{\text{III}}\text{-ENR}_3$  (Eq (5)) (Pignatello et al., 2006).

Due to this reason, under light at pH 3.0,  $\text{Fe}^{\text{III}}\text{-ENR}_3$  was even more reactive than ENR, obtaining 60% removal in 60 min, compared to the 40% of the free antibiotic (Fig. 4). By comparison to the photochemical system without  $\text{H}_2\text{O}_2$ , ENR removal effectiveness was increased by a factor of 2, while for  $\text{Fe}^{\text{III}}\text{-ENR}_3$ , this increment reached approximately a factor of 4.

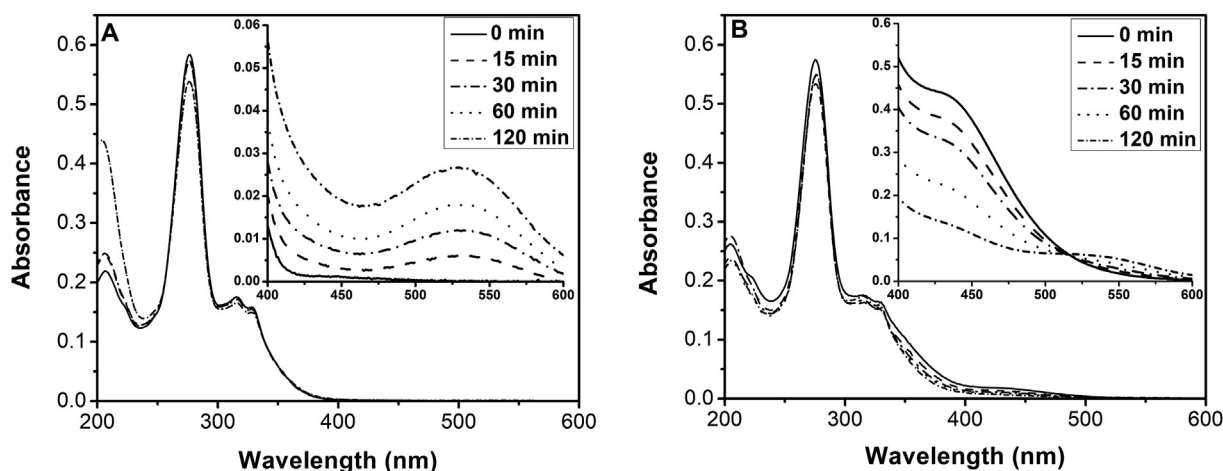
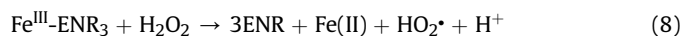


Fig. 3. Time-course absorbance spectra changes during irradiation experiments at pH 3.0. Full spectra were recorded by 20 times dilution of the original sample (in the insert). (A) ENR 300  $\mu\text{M}$ ; (B)  $\text{Fe}^{\text{III}}\text{-ENR}_3$  100  $\mu\text{M}$ .

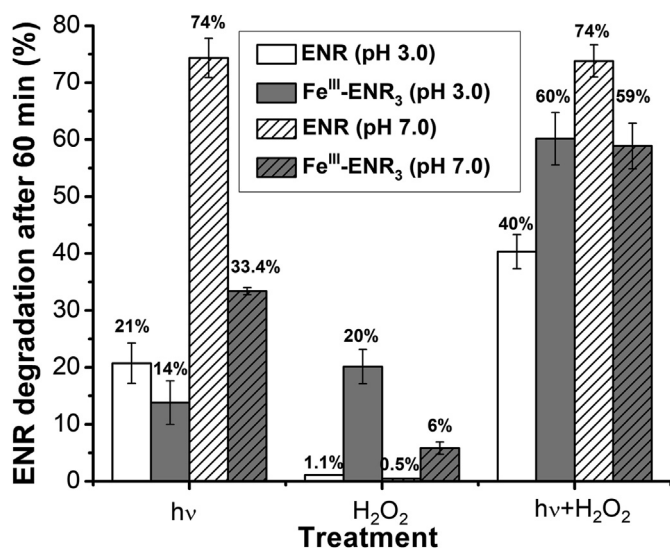


Fig. 4. Degradation percentages after 60 min at both studied pH in aerated conditions, under sunlight irradiation (h<sub>v</sub>), with H<sub>2</sub>O<sub>2</sub> 200 μM without irradiation (dark control), and the combination of both, h<sub>v</sub>+H<sub>2</sub>O<sub>2</sub> 200 μM, for 300 μM of ENR and 100 μM of Fe<sup>III</sup>-ENR<sub>3</sub>. Error bars were calculated as the associated standard deviation between respective duplicates.



At pH 7.0 under light, even though the antibiotic removal was slightly higher without Fe(III) (74% for the free form, and 59% for the iron complexed one in 60 min), H<sub>2</sub>O<sub>2</sub> did not enhance ENR degradation, thus, the contribution of the low concentration of photo-generated  $\cdot\text{OH}$  from H<sub>2</sub>O<sub>2</sub> photolysis was negligible for the already fast ENR photolytic degradation. On the contrary, the addition of H<sub>2</sub>O<sub>2</sub> to the analogous system containing Fe(III), represented a removal increment for almost the double than the one without it. Therefore, it can be hypothesized that photo-Fenton process was running even at pH 7.0, bearing in mind that is usually no longer effective in these conditions without the addition of any chelating agent due to the precipitation of iron oxides (De Luca et al., 2014; Huang et al., 2013; Santos-Juanes et al., 2017).

No significant differences were obtained for Fe<sup>III</sup>-ENR<sub>3</sub> under light and in the presence of H<sub>2</sub>O<sub>2</sub> for the both studied pH values (c.a. 60% in 60 min in both cases). However, since photolytic degradation was lower at pH 3.0 than at pH 7.0 (14% and 33% in 60 min, respectively), photo-Fenton contribution to the overall pollutant removal should have been lower at neutral conditions, as expected.

Within dark controls, the greater reactivity of Fe<sup>III</sup>-ENR<sub>3</sub> against H<sub>2</sub>O<sub>2</sub> was even more evident. While for ENR no degradation was observed in any case, for the iron-complex form, 20% degradation was achieved at pH 3.0, and 6% at pH 7.0.

### 3.4. Photoproduct identification and formation pathways

A total of 39 photoproducts were detected under the different reaction conditions, exact molecular formulas were determined for all of them, based on accurate mass measurements. The 14 most abundant ones were successfully isolated and fragmented to obtain structural information (Table S1), and a schematic degradation pathway was proposed (Fig. 5). Results for the whole 39 photoproducts are shown in Fig. S7.

Observing Fig. 6, since complexation reduced the direct photolysis of the FQ, lower photoproduct formation was obtained in the case of the iron-complex form at both studied pH without

H<sub>2</sub>O<sub>2</sub>. Analysing pH 3.0, photodegradation pathways did not differ significantly between ENR and Fe<sup>III</sup>-ENR<sub>3</sub>, observing in both cases that the main reaction was ethyl loss from piperazinyl ring, forming photoproduct A, ciprofloxacin (another commercial FQ), which is in agreement with related studies that have indicated it as the common path for ENR photolytic degradation (Li et al., 2011; Snowberger et al., 2016). Similarly, photoproduct C, still with no modification on the FQ core, presents rupture on the piperazinyl ring. Only in the cases of B, D, E and M, oxidation of chromophoric part of ENR became relevant. In addition, the use of IPA showed the expected decrease in formation of hydroxylated photoproducts (Fig. S7c), even though it had not significantly affected the pollutant degradation kinetics (Figs. S2a–b).

In sharp contrast with acidic conditions, at pH 7.0 without H<sub>2</sub>O<sub>2</sub>, photoproduct formation was notably distinctive when ENR was chelating iron compared to when it was not. In both cases, a higher variety of photoproducts were observed than the ones obtained at pH 3.0, presenting more defluorinated compounds (H, J, K, and N) and also decarboxylated (G, I and L). These reactions have been reported in the literature as common paths for FQ photolysis for zwitterionic chemical speciation form rather than for the cationic one (Sturini et al., 2012; Zhang et al., 2019). Moreover, in the case of Fe<sup>III</sup>-ENR<sub>3</sub>, fluorine substitution by hydroxyl group (photoproduct E) has been observed as the favored path, in contrast with the prevalent ciprofloxacin (photoproduct A) formation at pH 3.0. Without Fe(III) complexation, there was no formation of a single major photoproduct, but a wider variety of transformation products were detected in lower quantities.

It is well known that photo-induced decarboxylation reactions occur on Fe(III)-carboxylate complexes under sun-simulated irradiation (Abida et al., 2006; Passananti et al., 2016; Pignatello et al., 2006). However, in this case, lower decarboxylation was observed in the case of Fe<sup>III</sup>-ENR<sub>3</sub> than ENR, which is in agreement with previous observations reported in section 3.2.3, describing no significant iron loss during the 120 min of Fe<sup>III</sup>-ENR<sub>3</sub> irradiation at pH 7.0. This trend could be probably explained by the chelation mode between ENR and Fe(III) between the carbonyl and carboxyl groups of FQs, hence being an overall protection of the carboxylic acidic group. Nevertheless, the difference between the decarboxylation of ENR and Fe<sup>III</sup>-ENR<sub>3</sub> is the same as for the other photoproducts, obtaining maybe higher photoproduct formation for the non-complexed pollutant. Therefore, no conclusion can be taken from an enhancement or inhibition of decarboxylation between ENR and Fe<sup>III</sup>-ENR<sub>3</sub>.

When H<sub>2</sub>O<sub>2</sub> was added, at pH 3.0, formation of hydroxylated by-products (B, E and F) occurred at a higher extent in the case of Fe<sup>III</sup>-ENR<sub>3</sub>, which is in agreement with the higher  $\cdot\text{OH}$  production due to the photo-Fenton process. These differences are clearer when analysing the respective obtained photoproduct formation kinetics (Figs. S8a–b), noticing that not only the order of formation was different, but the rates as well. Interestingly, decarboxylation was negligible compared to direct photolysis (without H<sub>2</sub>O<sub>2</sub>), where D and M were obtained in higher amounts.

In the case of pH 7.0, the addition of H<sub>2</sub>O<sub>2</sub> did not alter the photodegradation mechanism of ENR compared to the results without the addition of it. On the other hand, despite the fact that with Fe<sup>III</sup>-ENR<sub>3</sub> differences were not as clear as the ones at pH 3.0, when analysing Figs. S7e–f, enhanced oxidized products were formed when H<sub>2</sub>O<sub>2</sub> was added, results that are in agreement with the ones shown in section 3.3.

## 4. Conclusions

Our results demonstrate that iron, ubiquitous metal in water compartment as well as catalyst reagent in photo-Fenton type

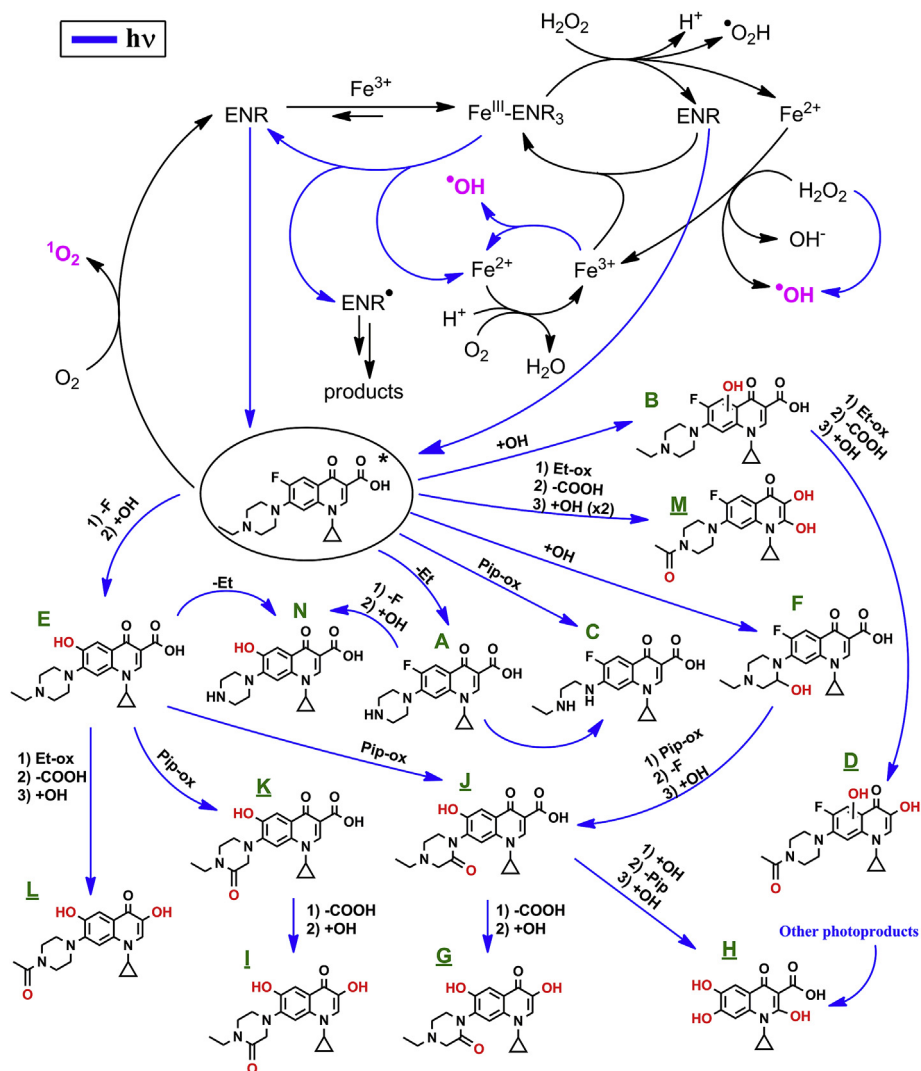


**Figure 5.** Summary of the studied reactions and photoproduct formation mechanism proposal. Underlined photoproducts were found for the first time in this work. Reactions include defluorination (-F), decarboxylation (-COOH), hydroxylation (+OH), piperazine cleavage and oxidation (-Pip and Pip-ox, respectively), and ethyl moiety cleavage and oxidation (-Et and Et-ox, respectively).

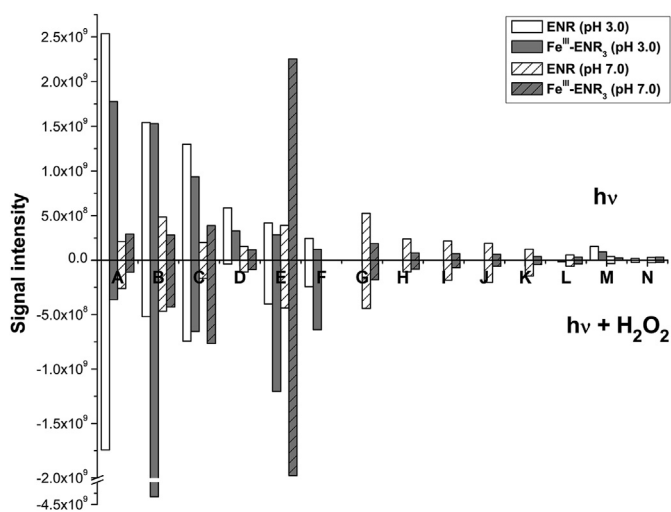


**Figure 6.** Obtained photoproducts formation after 120 min for ENR 300  $\mu$ M and Fe<sup>III</sup>-ENR<sub>3</sub> 100  $\mu$ M, pH 3.0 and 7.0. Above with only light irradiation (hv), and below with hv + H<sub>2</sub>O<sub>2</sub> 200  $\mu$ M.

processes, can strongly affect the photochemical processes of ENR also frequently found in aqueous media. Indeed, when iron, coexist with ENR, they form a stable complex within a wide pH range, affecting each other's photochemistry, in particular, decreasing ENR photolytic rate constant, thus probably enhancing their persistence in the environment. Photoproduct formation pathway is also affected by metal chelation. The FQ-Fe(III) complex was efficiently removed from water only with the addition of H<sub>2</sub>O<sub>2</sub>, due to photo-Fenton process. In this sense, even though FQs could be photochemically stabilized in the presence of Fe(III), this coexistence could represent an advantage when achieving Fenton-type treatment at circumneutral pH for the degradation of more recalcitrant pollutants.

### Author contribution

Iván Sciscenko - PhD Student, principal investigator: literature search (information about fluoroquinolones and its environmental relevance, related photochemical works, proposed degradation pathways, etc.), methodology (solution preparation, analytical measurements), experiments (formation of ENR-Fe complex,

irradiations in different described conditions), Formal analysis and comparison with other works, writing: Writing – original draft. Antonio Arques - Main PhD supervisor of Iván Sciscenko following the complete work: conceptualization, Supervision, Writing: review & editing. Zsuzsanna Varga – Implementation and optimization of the Mass Spectrometry experiments, analysis and preliminary data interpretation of Mass Spectrometry work: methodology, Investigation. Stephane Bouchonnet - Comprehensive structural elucidation of the transformation products of Enrofloxacin from ICR high-resolution mass spectrometry data: investigation, Formal analysis. Olivier Monfort – co-supervision of Iván Sciscenko in France (discussion and interpretation of obtained results), study of Fe-ENR complexation (characterization of physicochemical properties of Fe-ENR complex), set-up of photochemical experiments along with their interpretations (fate of Fe and ENR): methodology, writing: review & editing. Marcello Brigante - co-supervision of Iván Sciscenko in France more precisely on laser flash photolysis investigation, radical chemistry investigation: conceptualization, Supervision, Investigation, writing: Writing – original draft, writing: review & editing. Gilles Mailhot: Main supervisor of Iván Sciscenko in France, expert in water and iron chemistry and environmental photochemistry, analysis of data from iron complex and photochemical experiments and responsible of the work organization in Clermont-Ferrand (France): supervision, Conceptualization, writing: Writing – original draft, writing: review & editing.

### Declaration of competing interest

The authors declare that they have no known competing financial interests or personal relationships that could have appeared to influence the work reported in this paper.

### Acknowledgement

This paper is part of a project that has received funding from the European Union's Horizon 2020 research and innovation programme under the Marie Skłodowska-Curie grant agreement No. 765860 (AQUALity). The paper reflects only the authors' view and the Agency is not responsible for any use that may be made of the information it contains. M.B. and G. M. acknowledge financial support from the CAP 20–25 I-site project.

### Appendix A. Supplementary data

Supplementary data to this article can be found online at <https://doi.org/10.1016/j.chemosphere.2021.129791>.

### References

Abida, O., Mailhot, G., Litter, M., Bolte, M., 2006. Impact of iron-complex (Fe(III)-NTA) on photoinduced degradation of 4-chlorophenol in aqueous solution. *Photochem. Photobiol. Sci.* 5, 395–402. <https://doi.org/10.1039/b518211e>.

Albini, A., Monti, S., 2003. Photophysics and photochemistry of fluoroquinolones. *Chem. Soc. Rev.* 32, 238–250. <https://doi.org/10.1039/b209220b>.

Appiani, E., Ossola, R., Latch, D.E., Erickson, P.R., McNeill, K., 2017. Aqueous singlet oxygen reaction kinetics of furfuryl alcohol: effect of temperature, pH, and salt content. *Environ. Sci. Process. Impacts* 19, 507–516. <https://doi.org/10.1039/c6em00646a>.

Aristilde, L., Sposito, G., 2010. Binding of ciprofloxacin by humic substances: a molecular dynamics study. *Environ. Toxicol. Chem.* 29, 90–98. <https://doi.org/10.1002/etc.19>.

Batchu, S.R., Panditi, V.R., O'Shea, K.E., Gardinali, P.R., 2014. Photodegradation of antibiotics under simulated solar radiation: implications for their environmental fate. *Sci. Total Environ.* 470–471, 299–310. <https://doi.org/10.1016/j.scitotenv.2013.09.057>.

Bianco, A., Passananti, M., Perroux, H., Voyard, G., Mouchel-Vallon, C., Chaumerliac, N., Mailhot, G., Deguillaume, L., Brigante, M., 2015. A better understanding of hydroxyl radical photochemical sources in cloud waters

collected at the puy de Dôme station - experimental versus modelled formation rates. *Atmos. Chem. Phys.* 15, 9191–9202. <https://doi.org/10.5194/acp-15-9191-2015>.

Bokare, A.D., Choi, W., 2015. Singlet-oxygen generation in alkaline periodate solution. *Environ. Sci. Technol.* 49, 14392–14400. <https://doi.org/10.1021/acs.est.5b04119>.

Bucheli-Witschel, M., Egli, T., 2001. Environmental fate and microbial degradation of aminopolycarboxylic acids. *FEMS Microbiol. Rev.* 25, 69–106. [https://doi.org/10.1016/S0168-6445\(00\)00055-3](https://doi.org/10.1016/S0168-6445(00)00055-3).

Buxton, G.V., Greenstock, C.L., Helman, W.P., Ross, A.B., 1988. Critical Review of rate constants for reactions of hydrated electrons, hydrogen atoms and hydroxyl radicals ( $\cdot\text{OH}/\cdot\text{O}$ ) in Aqueous Solution. *J. Phys. Chem. Ref. Data* 17, 513–886. <https://doi.org/10.1063/1.555805>.

Chen, Y., Wang, A., Zhang, Y., Bao, R., Tian, X., Li, J., 2017. Electro-Fenton degradation of antibiotic ciprofloxacin (CIP): formation of Fe $^{3+}$ -CIP chelate and its effect on catalytic behavior of Fe $^{2+}$ /Fe $^{3+}$  and CIP mineralization. *Electrochim. Acta* 256, 185–195. <https://doi.org/10.1016/j.electacta.2017.09.173>.

Cuprys, A., Pulicharla, R., Brar, S.K., Drogui, P., Verma, M., Surampalli, R.Y., 2018. Fluoroquinolones metal complexation and its environmental impacts. *Coord. Chem. Rev.* 376, 46–61. <https://doi.org/10.1016/j.ccr.2018.05.019>.

De Luca, A., Dantas, R.F., Esplugas, S., 2014. Assessment of iron chelates efficiency for photo-Fenton at neutral pH. *Water Res.* 61, 232–242. <https://doi.org/10.1016/j.watres.2014.05.033>.

Efthimiadou, E.K., Karaliota, A., Psomas, G., 2008. Mononuclear metal complexes of the second-generation quinolone antibacterial agent enrofloxacin: synthesis, structure, antibacterial activity and interaction with DNA. *Polyhedron* 27, 1729–1738. <https://doi.org/10.1016/j.poly.2008.02.006>.

Ge, L., Halsall, C., Chen, C.E., Zhang, P., Dong, Q., Yao, Z., 2018. Exploring the aquatic photodegradation of two ionisable fluoroquinolone antibiotics – gatifloxacin and balofloxacin: degradation kinetics, photoproducts and risk to the aquatic environment. *Sci. Total Environ.* 633, 1192–1197. <https://doi.org/10.1016/j.scitotenv.2018.03.279>.

Ge, L., Na, G., Zhang, S., Li, K., Zhang, P., Ren, H., Yao, Z., 2015. New insights into the aquatic photochemistry of fluoroquinolone antibiotics: direct photodegradation, hydroxyl-radical oxidation, and antibacterial activity changes. *Sci. Total Environ.* 527 (528), 12–17. <https://doi.org/10.1016/j.scitotenv.2015.04.099>.

Gou, Y., Chen, P., Yang, L., Li, S., Peng, L., Song, S., Xu, Y., 2020. Degradation of fluoroquinolones in homogeneous and heterogeneous photo-Fenton processes: a review. *Chemosphere* 129481. <https://doi.org/10.1016/j.chemosphere.2020.129481>.

Haag, W.R., Hoigné, J., Gassman, E., Braun, A.M., 1984. Singlet oxygen in surface waters - Part I: furfuryl alcohol as a trapping agent. *Chemosphere* 13, 631–640. [https://doi.org/10.1016/0045-6535\(84\)90199-1](https://doi.org/10.1016/0045-6535(84)90199-1).

Haag, W.R., Mill, T., 1987. Rate constants for interaction of 1O $_{21}\Delta$ g with azide ion in water. *Photochem. Photobiol.* 45, 317–321. <https://doi.org/10.1111/j.1751-1097.1987.tb05381.x>.

Haddad, T., Kümmerer, K., 2014. Characterization of photo-transformation products of the antibiotic drug Ciprofloxacin with liquid chromatography-tandem mass spectrometry in combination with accurate mass determination using an LTQ-Orbitrap. *Chemosphere* 115, 40–46. <https://doi.org/10.1016/j.chemosphere.2014.02.013>.

Hamad, B., 2010. The antibiotics market. *Nat. Rev. Drug Discov.* 9, 675–676. <https://doi.org/10.1038/nrd3267>.

Huang, W., Bianco, A., Brigante, M., Mailhot, G., 2018. UVA-UVB activation of hydrogen peroxide and persulfate for advanced oxidation processes: efficiency, mechanism and effect of various water constituents. *J. Hazard Mater.* 347, 279–287. <https://doi.org/10.1016/j.jhazmat.2018.01.006>.

Huang, W., Brigante, M., Wu, F., Mousty, C., Hanna, K., Mailhot, G., 2013. Assessment of the Fe(III)-EDDS complex in Fenton-like processes: from the radical formation to the degradation of bisphenol A. *Environ. Sci. Technol.* 47, 1952–1959. <https://doi.org/10.1021/es304502y>.

Hubicka, U., Krzek, J., Zurowska, B., Walczak, M., Zylowski, M., Pawłowski, D., 2012. Determination of photostability and photodegradation products of moxifloxacin in the presence of metal ions in solutions and solid phase. Kinetics and identification of photoproducts. *Photochem. Photobiol. Sci.* 11, 351–357. <https://doi.org/10.1039/c1pp05259d>.

Kümmerer, K., 2009. The presence of pharmaceuticals in the environment due to human use - present knowledge and future challenges. *J. Environ. Manag.* 90, 2354–2366. <https://doi.org/10.1016/j.jenvman.2009.01.023>.

Latch, D.E., Stender, B.L., Packer, J.L., Arnold, W.A., McNeill, K., 2003. Photochemical fate of pharmaceuticals in the environment: cimetidine and ranitidine. *Environ. Sci. Technol.* 37, 3342–3350. <https://doi.org/10.1021/es0340782>.

Li, Y., Niu, J., Wang, W., 2011. Photolysis of Enrofloxacin in aqueous systems under simulated sunlight irradiation: kinetics, mechanism and toxicity of photolysis products. *Chemosphere* 85, 892–897. <https://doi.org/10.1016/j.chemosphere.2011.07.008>.

Miralles-Cuevas, S., Oller, I., Pérez, J.A.S., Malato, S., 2014. Removal of pharmaceuticals from MWTP effluent by nanofiltration and solar photo-Fenton using two different iron complexes at neutral pH. *Water Res.* 64, 23–31. <https://doi.org/10.1016/j.watres.2014.06.032>.

Niu, X.Z., Moore, E.G., Croué, J.P., 2018. Excited triplet state interactions of fluoroquinolone norfloxacin with natural organic matter: a laser spectroscopy study. *Environ. Sci. Technol.* 52, 10426–10432. <https://doi.org/10.1021/acs.est.8b02835>.

Passananti, M., Vinatier, V., Delort, A.M., Mailhot, G., Brigante, M., 2016.

- Siderophores in cloud waters and potential impact on atmospheric chemistry: photoreactivity of iron complexes under sun-simulated conditions. *Environ. Sci. Technol.* 50, 9324–9332. <https://doi.org/10.1021/acs.est.6b02338>.
- Pignatello, J.J., Oliveros, E., MacKay, A., 2006. Advanced oxidation processes for organic contaminant destruction based on the fenton reaction and related chemistry. *Crit. Rev. Environ. Sci. Technol.* 36, 1–84. <https://doi.org/10.1080/10643380500326564>.
- Qiu, W., Zheng, M., Sun, J., Tian, Y., Fang, M., Zheng, Y., Zhang, T., Zheng, C., 2019. Photolysis of enrofloxacin, pefloxacin and sulfaquinoxaline in aqueous solution by UV/H<sub>2</sub>O<sub>2</sub>, UV/Fe(II), and UV/H<sub>2</sub>O<sub>2</sub>/Fe(II) and the toxicity of the final reaction solutions on zebrafish embryos. *Sci. Total Environ.* 651, 1457–1468. <https://doi.org/10.1016/j.scitotenv.2018.09.315>.
- Renny, J.S., Tomasevich, L.L., Tallmadge, E.H., Collum, D.B., 2013. Method of continuous variations: applications of job plots to the study of molecular associations in organometallic chemistry. *Angew. Chem. Int. Ed.* 52, 11998–12013. <https://doi.org/10.1002/anie.201304157>.
- Riaz, L., Mahmood, T., Khalid, A., Rashid, A., Ahmed Siddique, M.B., Kamal, A., Coyne, M.S., 2018. Fluoroquinolones (FQs) in the environment: a review on their abundance, sorption and toxicity in soil. *Chemosphere* 191, 704–720. <https://doi.org/10.1016/j.chemosphere.2017.10.092>.
- Salimi, M., Esrafil, A., Gholami, M., Jonidi Jafari, A., Rezaei Kalantary, R., Farzadkia, M., Kermani, M., Sobhi, H.R., 2017. Contaminants of emerging concern: a review of new approach in AOP technologies. *Environ. Monit. Assess.* 189 <https://doi.org/10.1007/s10661-017-6097-x>.
- Santos-Juanes, L., Amat, A.A., Arques, A., 2017. Strategies to drive photo-fenton process at mild conditions for the removal of xenobiotics from aqueous systems. *Curr. Org. Chem.* 21, 1074–1083. <https://doi.org/10.2174/1385272821666170102150337>.
- Sciscenko, I., Garcia-Ballesteros, S., Sabater, C., Castillo, M.A., Escudero-Oñate, C., Oller, I., Arques, A., 2020. Monitoring photolysis and (solar photo)-Fenton of enrofloxacin by a methodology involving EEM-PARAFAC and bioassays: role of pH and water matrix. *Sci. Total Environ.* 719, 137331. <https://doi.org/10.1016/j.scitotenv.2020.137331>.
- Silva, B.F. da, Jelic, A., López-Serna, R., Mozeto, A.A., Petrovic, M., Barceló, D., 2011. Occurrence and distribution of pharmaceuticals in surface water, suspended solids and sediments of the Ebro river basin, Spain. *Chemosphere* 85, 1331–1339. <https://doi.org/10.1016/j.chemosphere.2011.07.051>.
- Snowberger, S., Adejumo, H., He, K., Mangalgi, K.P., Hopanna, M., Soares, A.D., Blaney, L., 2016. Direct photolysis of fluoroquinolone antibiotics at 253.7 nm: specific reaction kinetics and formation of equally potent fluoroquinolone antibiotics. *Environ. Sci. Technol.* 50, 9533–9542. <https://doi.org/10.1021/acs.est.6b01794>.
- Stefánsson, A., 2007. Iron(III) hydrolysis and solubility at 25°C. *Environ. Sci. Technol.* 41, 6117–6123. <https://doi.org/10.1021/es070174h>.
- Sturini, M., Speltini, A., Maraschi, F., Profumo, A., Pretali, L., Fasani, E., Albini, A., 2010. Photochemical degradation of marbofloxacin and enrofloxacin in natural waters. *Environ. Sci. Technol.* 44, 4564–4569. <https://doi.org/10.1021/es100278n>.
- Sturini, M., Speltini, A., Maraschi, F., Profumo, A., Pretali, L., Irastorza, E.A., Fasani, E., Albini, A., 2012. Photolytic and photocatalytic degradation of fluoroquinolones in untreated river water under natural sunlight. *Appl. Catal. B Environ.* 119–120, 32–39. <https://doi.org/10.1016/j.apcatb.2012.02.008>.
- Tao, Y., Brigante, M., Zhang, H., Mailhot, G., 2019. Phenanthrene degradation using Fe(III)-EDDS photoactivation under simulated solar light: a model for soil washing effluent treatment. *Chemosphere* 236, 124366. <https://doi.org/10.1016/j.chemosphere.2019.124366>.
- Uivarosi, V., 2013. Metal complexes of quinolone antibiotics and their applications: an update. *Molecules* 18, 11153–11197. <https://doi.org/10.3390/molecules180911153>.
- Urbaniak, B., Kokot, Z.J., 2009. Analysis of the factors that significantly influence the stability of fluoroquinolone-metal complexes. *Anal. Chim. Acta* 647, 54–59. <https://doi.org/10.1016/j.aca.2009.05.039>.
- Van Doorslaer, X., Dewulf, J., Van Langenhove, H., Demeestere, K., 2014. Fluoroquinolone antibiotics: an emerging class of environmental micropollutants. *Sci. Total Environ.* 500–501, 250–269. <https://doi.org/10.1016/j.scitotenv.2014.08.075>.
- Verlicchi, P., Al Aukidy, M., Zambello, E., 2012. Occurrence of pharmaceutical compounds in urban wastewater: removal, mass load and environmental risk after a secondary treatment-A review. *Sci. Total Environ.* 429, 123–155. <https://doi.org/10.1016/j.scitotenv.2012.04.028>.
- Vermilyea, A.W., Voelker, B.M., 2009. Photo-fenton reaction at near neutral pH. *Environ. Sci. Technol.* 43, 6927–6933. <https://doi.org/10.1021/es900721x>.
- Wang, S., Wang, Z., Hao, C., Peijnenburg, W.J.G.M., 2018. DFT/TDDFT insights into effects of dissociation and metal complexation on photochemical behavior of enrofloxacin in water. *Environ. Sci. Pollut. Res.* 25, 30609–30616. <https://doi.org/10.1007/s11356-018-3032-9>.
- Wei, X., Chen, J., Xie, Q., Zhang, S., Li, Y., Zhang, Y., Xie, H., 2015. Photochemical behavior of antibiotics impacted by complexation effects of concomitant metals: a case for ciprofloxacin and Cu(II). *Environ. Sci. Process. Impacts* 17, 1220–1227. <https://doi.org/10.1039/c5em00204d>.
- Zhang, Z., Xie, X., Yu, Z., Cheng, H., 2019. Influence of chemical speciation on photochemical transformation of three fluoroquinolones (FQs) in water: kinetics, mechanism, and toxicity of photolysis products. *Water Res.* 148, 19–29. <https://doi.org/10.1016/j.watres.2018.10.027>.